Compact Multi-harmonic Suppression LTCC Bandpass Filter Using Parallel Short-Ended Coupled-Line Structure

Xu-Guang Wang, Young Yun, and In-Ho Kang

This paper presents a novel simple filter design method based on a parallel short-ended coupled-line structure with capacitive loading for size reduction and ultra-broad rejection of spurious passbands. In addition, the introduction of a cross-coupling capacitor into the miniaturized coupled-line can create a transmission zero at the second harmonic frequency for better frequency selectivity and attenuation level. The aperture compensation technique is also applied to achieve a strong coupling in the coupled-line section. The influence of using the connecting transmission line to cascade two identical one-stage filters is studied for the first time. Specifically, such a two-stage bandpass filter operating at 2.3 GHz with a fractional bandwidth of 10% was designed and realized with low-temperature co-fired ceramic technology for application in base stations that need high power handling capability. It achieved attenuation in excess of -40 dB up to $4f_0$ and low insertion loss of -1.2 dB with the size of 10 mm × 7 mm × 2.2 mm. The measured and simulated results showed good agreement.

Keywords: Harmonic suppression, coupled-line, bandpass filter, LTCC.

I. Introduction

In recent years, compact, high-performance, and low-cost components for radio frequency (RF) applications have been the focus of a great deal of research and industrial pursuit with the explosive growth of modern wireless communication services. One promising method for many miniaturizing and packaging technologies [1]-[3] is to use low-temperature co-fired ceramic (LTCC) [4], [5] on account of its multilayer structure and high unloaded quality factor.

The bandpass filter is an essential component in the RF front-end of communication systems. It passes the desired frequencies, rejects unwanted signals, and suppresses harmonics. However, as a result of the distributed characteristic of the transmission line, undesired spurious passbands or harmonics are a problem for conventional filters and can seriously degrade their performance, which may be critical in certain applications. To find a way to suppress spurious responses, many studies have been carried out. Using the technique of photonic bandgap (PBG) and defected ground structure (DGS) is one of the most popular approaches.

The PBG structure was initially proposed in the optical field, and essentially comprises periodic etched defects on the back of a metallic ground plane which can provide effective and flexible control of the propagation of electromagnetic (EM) waves along a specific direction or in all directions. Since it was applied to microwave and millimeter frequency-band applications, numerous novel PBG structures have been proposed for the design of both passive and active devices with the property of multi-harmonic suppression [6]-[9]. However,

the PBG structure has modeling difficulties because there are too many design parameters that have an effect on the bandgap property, such as the number of lattices, lattice shapes, lattice spacing, and relative volume fraction. Another difficulty in using the PBG circuit is caused by the radiation from the periodic etched defects [10]. The DGS with periodic or non-periodic arrays is another very practical approach because it can provide a rejection band in some frequency ranges. Compared with the PBG structure, which needs many units to build a filter, the DGS is simpler because only a few units can be used to construct a filter, and this results in a smaller filter size. The rejection characteristic of the DGS is available to many microwave circuits, such as power-amplifier modules, planar antennas, power dividers and filters, and so on [11]-[14]. However, due to the periodic structure of the PBG and DGS, these filters suffer from their large circuit areas and specific circuit configurations, which seriously hinder their application to wireless communication systems.

In this paper, we propose a compact multi-harmonic suppression LTCC bandpass filter based on the capacitive loading of the parallel short-ended coupled-line structure. This is a relatively simple way of reducing the coupled-line electrical length, which usually plays a decisive role in the filter size. On the other hand, the use of lumped elements can effectively suppress the spurious passbands. In addition, the cross-coupling capacitor and aperture compensation technique are employed for better performance. Such a compact two-stage bandpass filter working at 2.3 GHz with high power handling capability was implemented in a multilayer LTCC substrate and examined carefully. In addition to the advantage of excellent multi-harmonic suppression (better than -40 dB up to $4f_0$) where f_0 is the center frequency, the fabricated bandpass filter has a small size of 10 mm × 7 mm × 2.2 mm and low insertion loss of -1.2 dB.

II. Design Theory

1. Size Reduction Method

Figure 1(a) shows the generalized bandpass filter structure to be miniaturized in this design. The admittance inverter, which is a quarter-wavelength transmission line with characteristic impedance $Z_0 = 50\ \Omega$, can be replaced with a lumped circuit as shown in Fig. 1(b), where C_1 and L_1 are the equivalent lumped capacitance and inductance, respectively, and the value of C_1 is given by

$$C_1 = \frac{1}{\omega Z_0}. \qquad (1)$$

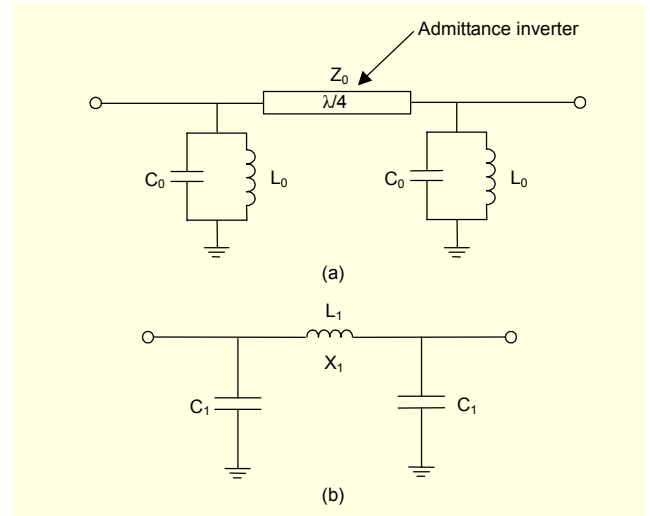Then, we have Fig. 2(a), in which the dotted network can

Fig. 1. (a) Schematic of the generalized bandpass filter used in this design and (b) the equivalent lumped circuit of the quarter-wavelength transmission line.
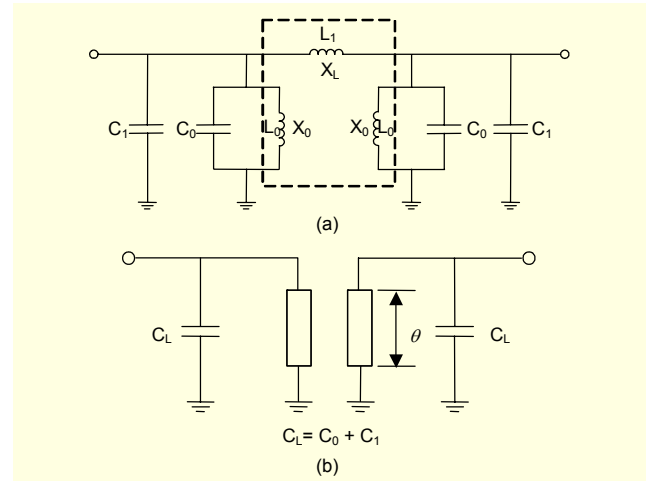

Fig. 2. (a) Equivalent lumped circuit of the generalized bandpass filter and (b) its miniaturized configuration based on the parallel short-ended coupled-line with capacitive loading.

be further made equivalent to the parallel short-ended coupled-line section with electrical length of θ when the following are satisfied as in [15]:

$$X_0 = Z_{0e}\tan\theta, \qquad (2)$$

$$X_L = \frac{2Z_{0e}Z_{0o}}{Z_{0e} - Z_{0o}}\tan\theta, \qquad (3)$$

where Z_{0e} and Z_{0o} are even- and odd-mode impedances of the coupled-line, respectively.

Figure 2(b) shows the miniaturized filter configuration based on the transformation described above and the value of C_0 can be deduced from (2) as

$$C_0 = \frac{1}{\omega Z_{0e} \tan\theta} . \qquad (4)$$

2. Improvement of the Filter Performance

The attenuation level at the second harmonic frequency can be further improved by employing the cross-coupling capacitor C_C in the miniaturized coupled-line section as shown in Fig. 3(a), which can create a transmission zero such that a sharper falloff rate at the right passband edge is obtained. The presence of this transmission zero (as long as it is not too close to the passband) does not change the passband characteristics of the filter too much. Figure 3(b) shows the equivalent lumped circuit of the final miniaturized one-stage bandpass filter, from which we can see that it is the dotted resonator that creates the transmission zero in the upper stopband. Therefore, the location of this transmission zero may easily be adjusted by varying the capacitor value.

Figure 4 shows the simulated filter responses for different values of the capacitor C_C. With nearly the same passband performance, the attenuation poles are located at the frequencies of 3.3 GHz, 3.9 GHz, 4.6 GHz, and 5.5 GHz when the capacitor values are 1.5 pF, 0.8 pF, 0.5 pF, and 0.3 pF, respectively. However, it should be noted that the stopband attenuation levels differ in these different cases.

By selecting the capacitor value properly, it can be designed to achieve a transmission zero to suppress the second harmonic with same passband response as the proposed filter in the previous subsection. Furthermore, this transmission zero can
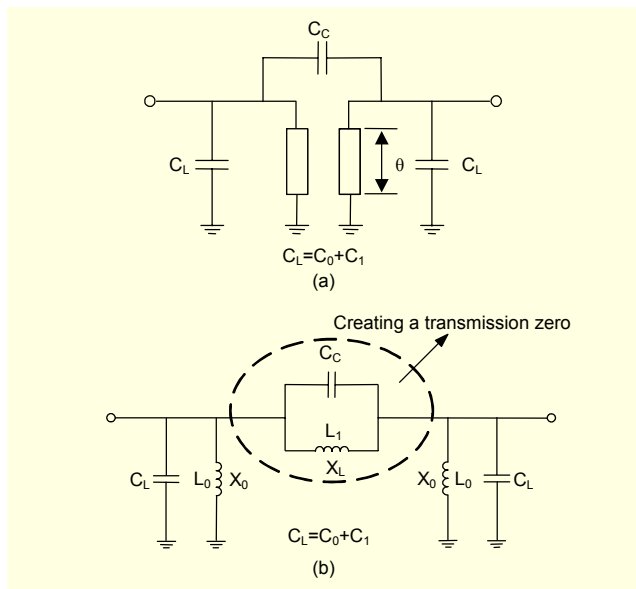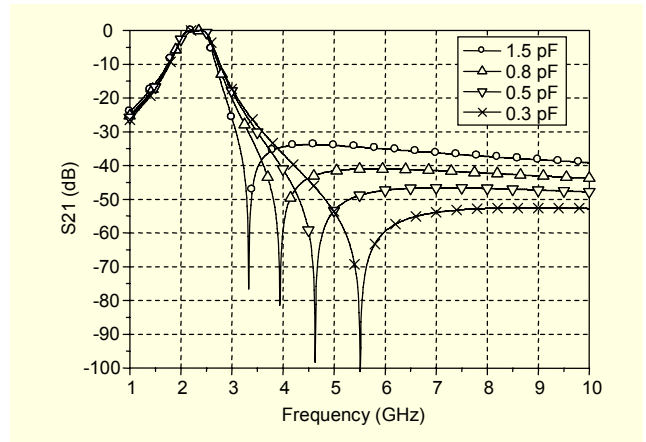
Fig. 4. Simulated frequency responses for various cross-coupling capacitors in ADS.
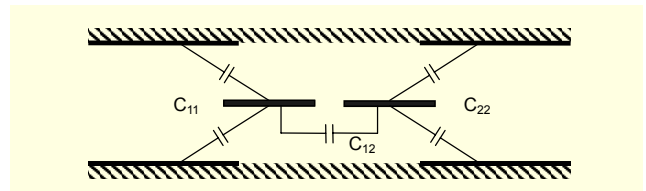
Fig. 5. Equivalent capacitance network of the coupled striplines.

also suppress the spurious response resulting from cascading as explained in detail in the next section.

Note that the insertion of this cross-coupling capacitor will change the coupling situation of the coupled-line. In the proposed design, it is coupled both electromagnetically and electrically through C_C, whereas the initial coupled-line is coupled only electromagnetically. Consequently, some modifications of the parameters of the coupled-line are necessary. This is not a troublesome problem since we can use Agilent's Advanced Design System (ADS) to find the proper new parameters quickly, which will also be expounded in detail in the next section. In this case, the spacing between two strip conductors is usually smaller than that for a conventional parallel coupled-line, which means that the EM coupling is larger.

However, the narrow spacing may only be reduced to a certain extent due to the limitation of fabricating tolerance. To relieve this limitation and realize a tightly coupled section, the aperture compensation technique is applied in this study. Figure 5 shows a schematic layout of the coupled striplines in which a wide aperture with rectangular configuration is formed on both ground planes over and underneath the coupled striplines in the center. This aperture has an effect on the equivalent capacitances between the strip conductors and the ground as shown in Fig. 5. With this aperture, the even-mode characteristic of the coupled striplines increases as the effective

Fig. 3. (a) Final structure of the miniaturized one-stage bandpass filter with a transmission zero and (b) its equivalent lumped circuit.

Table 1. Specifications of the proposed two-stage bandpass filter.

Center frequency	2.3 GHz
Fractional bandwidth	10%
Insertion loss	-1.5 dB maximum
Stopband rejection	< -60 dB up to $3f_0$

Fig. 6. Simulated frequency responses of both the initial miniaturized bandpass filter and its modified version in ADS.

distance between the strip conductors and the ground increases [16] as seen in Fig. 5. However, the odd-mode characteristic remains nearly the same because its value is mainly determined by C_{12} which is barely influenced by the aperture. As a result, coupling coefficient K could be increased tremendously.

III. Filter Implementation with LTCC Technology

Table 1 gives the specifications of the desired compact two-stage bandpass filter. The first step was to obtain the circuit parameters of the one-stage filter according to the desired specifications and fine tune each element value. Then, two identically tuned filters were cascaded through a short connecting transmission line [17]. After converting the circuit parameters to physical filter structures, some necessary tuning and optimizations were carried out to accommodate the parasitic effects of each lumped element, mutual coupling effects between elements, and to finalize the layout design by employing a full-wave EM simulation tool. Finally, the designed bandpass filter was fabricated with multilayer LTCC technology and carefully examined. To design the filters in a time-efficient way, we adopted both the circuit simulation software Agilent ADS and the full-wave 3-D EM simulation tool Ansoft HFSS to expedite the otherwise difficult work.

1. Circuit Simulation

First, a one-stage bandpass filter was designed to have a center frequency of 2.3 GHz with a fractional bandwidth of 10%. The electrical length of the short-ended coupled-line was chosen as 10º. Depending on the arbitrary selection of even-mode impedance Z_{0e} as 60 Ω, the value of the lumped capacitor C_L was calculated to be 7.9 pF using (1) and (4). The corresponding odd-mode impedance of the coupled-line Z_{0o} was 42 Ω, making the coupling coefficient K of the short-ended coupled-line 0.18. The bandwidth of this proposed filter depends on the coupling coefficient K. When K increases, the bandwidth becomes broader, and vice versa [18]. Therefore, the bandwidth of the filter can be controlled by varying the coupling coefficient when the quarter-wavelength transmission line is miniaturized. However, the broad bandwidth leads to a
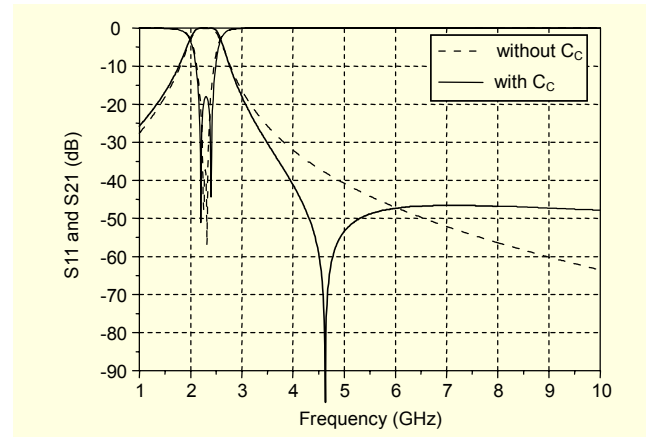
large coupling coefficient K, and accordingly, there is a great difference between Z_{0e} and Z_{0o}, which results in a large electrical length of the coupled-line. Therefore, a necessary design trade-off between broad bandwidth and small circuit size should be considered.

Then, the cross-coupling capacitor C_C was inserted to realize a transmission zero at 4.6 GHz for better upper skirt characteristic and second harmonic suppression. As previously mentioned, the insertion of C_C leads to tight coupling; thus, we have to decrease the odd-mode impedance Z_{0o} of the coupled-line and keep the even-mode impedance the same. The resulting circuit can be optimized with ADS to achieve the desired filter responses. This optimization process is very time-efficient because it is a lumped element circuit simulation. Here, the cross-coupling capacitor C_C of 0.5 pF and the odd-mode impedance Z_{0o} of 36.6 Ω are the optimum values in this design.

The ADS simulated results of the initial miniaturized filter and its modified version are plotted and compared in Fig. 6. Obviously, without affecting the fundamental frequency response, the modified filter performance achieved significant improvement as we expected by trading off the attenuation level at the far end of the upper stopband and no spurious response appeared.

The final two-stage bandpass filter can be achieved by simply connecting two identical obtained circuits using a short transmission line. However, this connecting line will generate an extra spurious response unless its electrical length is $0°$, which is impossible in the practical situation. Figures 7(a) and (b) show the spurious response in both cases of cascading the initial miniaturized one-stage bandpass filter and cascading its modified version with a transmission zero.

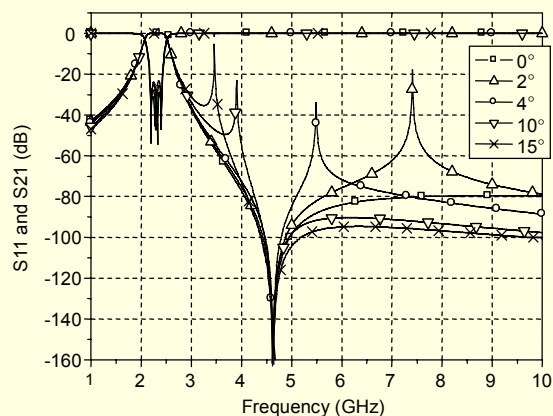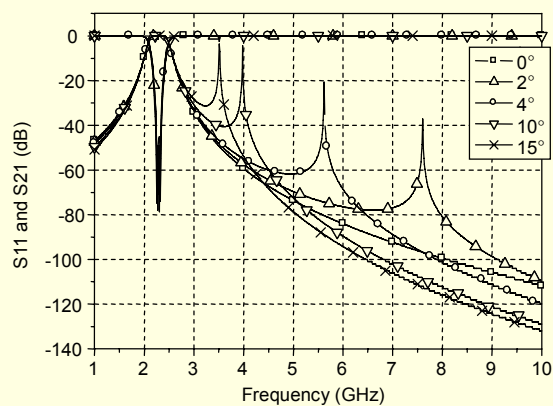Specific studies on the connecting transmission line have

Fig. 7. Spurious response resulting from the connecting transmission line: (a) cascading the initial miniaturized one-stage bandpass filter and (b) cascading its modified version with a transmission zero.
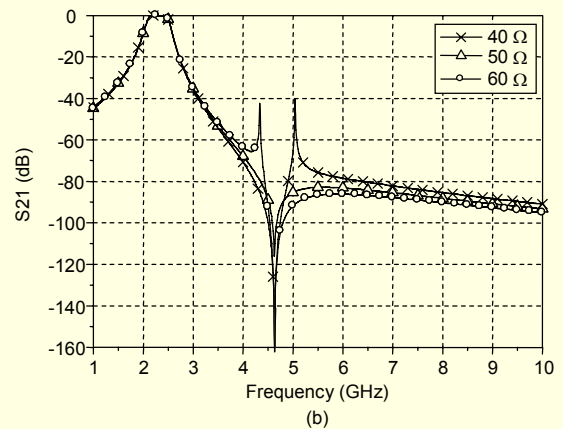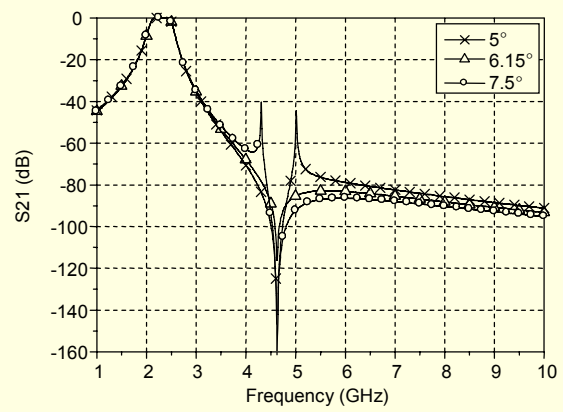
Fig. 8. Simulated frequency responses in ADS according to (a) the electrical length of the connecting line and (b) the impedance of the connecting line.

been done with ADS. It has been found that the location of this spurious band is closely related to the electrical length and the impedance of the connecting line; thus, we can shift the peak of the spurious band to the transmission zero frequency to suppress it.

Figure 8(a), which gives the simulated results for various electrical lengths of the connecting line with the same impedance of 50 Ω, indicates that a longer electrical length causes the spurious band peak to shift to a lower frequency. Figure 8(b) shows the frequency response in response to various impedances of the connecting line with the same electrical length of 6.15°. It can be seen that as the impedance of the connecting transmission line gets higher, the peak of the spurious band moves to a lower frequency. Therefore, based on the simulation results, a connecting transmission line with an electrical length of 6.15° and an impedance of 50 Ω, which can move the peak of the spurious band to the second harmonic frequency, is adopted to make the undesired spurious band disappear in this design.

2. Full-Wave EM Simulation and Optimization

Once the bandpass filter equivalent circuit model was developed, physical filter structures such as resonators and coupled-line sections could be designed. However, it is important to note that the synthesized filter model could not be transformed into physical structures at one time due to parasitic components (both internally and externally). As a result, either an optimization of the physical filter dimensions or a tuning of the filter responses is necessary. Usually, this is carried out using Ansoft HFSS until the EM simulation shows a performance close to the target one.

As in the simulation procedure in ADS, a one-stage bandpass filter was first implemented in a seven-layer LTCC substrate, which has a dielectric constant of 5.6 and a metal thickness of 15 μm. The distances between the metal layers are 585, 650, 20, 20, 650, and 200 μm consecutively from the top. Figure 9(a) displays the 3-D physical architecture. The parallel coupled-line is realized at layer 4 using stripline form because the dispersion and radiation of the stripline are negligible, and the upper and lower ground planes provide effective shielding. The
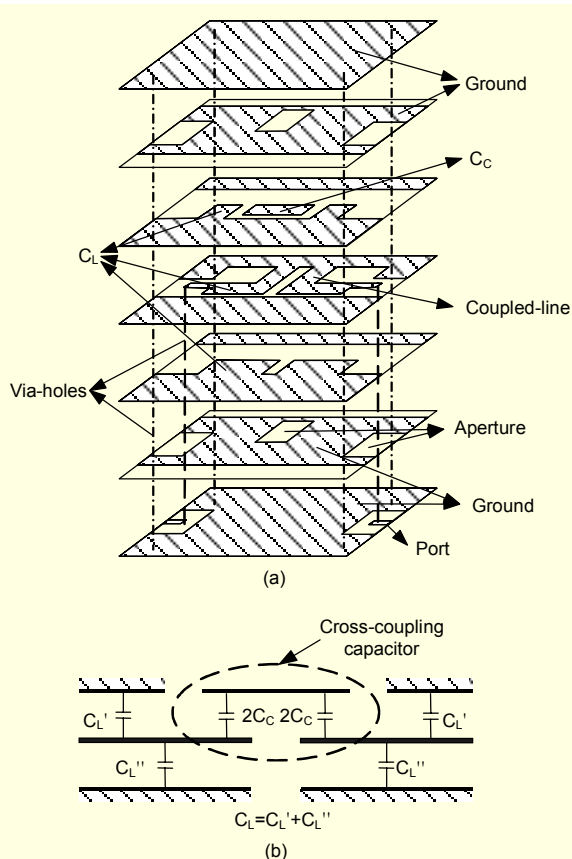
Fig. 9. (a) LTCC layout of the designed one-stage bandpass filter and (b) the detailed capacitor configuration.

Fig. 10. 3-D view of the PCB environment.

Fig. 11. HFSS simulated results of the designed one-stage bandpass filter with a small PCB.

capacitors are implemented on layers 3, 4, and 5 using the simple metal-insulator-metal structure. The detailed capacitor configuration schematic is shown in Fig. 9(b). Layers 2 and 6 are the stripline ground with rectangular configuration apertures over and underneath the coupled striplines. The minimum spacing between the coupled stripline conductors with the screen-printing LTCC process limits the ability to make the desired tighter coupling. So this design resorts to the aperture compensation technique to overcome this problem. The top and bottom grounds shield the filter, which minimizes the interaction with other components, while the surrounding ground located on layer 4 has the same effect. Such a large ground area can also improve the heat dissipation and high power handling capability. All of the ground layers are connected with the aid of two rows of periodic metalized via-holes with a diameter of 200 μm. Since the input and output ports are located at the bottom layer, they are also connected to the resonators by via-holes. Silver is used for both the strip conductor and the via-hole conductor. Note that the internal grounds at layers 2 and 6 cannot occupy the entire area in both margins according to the LTCC process design rule that they should be less than a certain percentage.
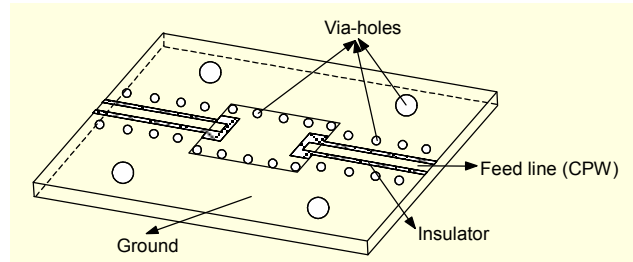
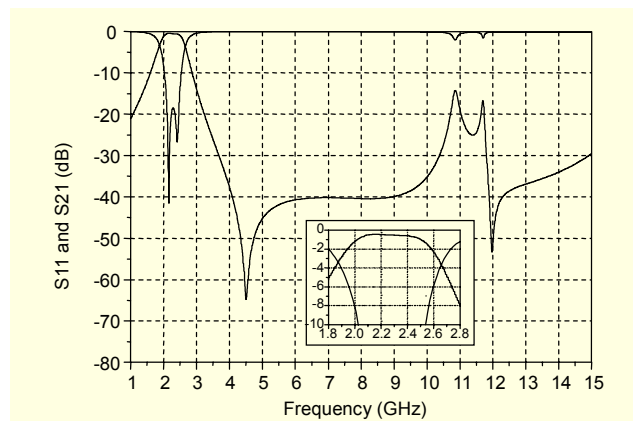Considering the practical environment, the LTCC bandpass filter is mounted on the pad of a PCB as shown in Fig. 10, with the signal feed composed of coplanar waveguide (CPW) feed lines printed on the top of the PCB. Thus, the overall performance should include the parasitic effect of the PCB. The one-stage filter responses, including a small PCB with a feed line of 500 μm, after optimization in HFSS are given in Fig. 11. To show the details in the passband, an inset graph is also presented. Excellent agreement between the ADS simulation and the HFSS simulation can be observed, including a very low insertion loss of -0.55 ± 0.1 dB, good rejection at $2f_0$ due to the transmission zero, and wide stopband rejection of about -40 dB up to 10 GHz. It is believed that the stopband rejection level can be enhanced by cascading more stages.

After the geometrical parameters of the coupled-line, capacitors, and ground plane apertures were obtained by fine tuning in HFSS, cascading was carried out for the final step. As can be seen from the top view of layer 4 in Fig. 12, two identical one-stage filters were reversely connected by a short transmission line to place the ports in the center.

The filter responses simulated by HFSS are shown in Fig. 13, and the detailed passband responses are also plotted in the inset graph. This simulation was also carried out including a small PCB with a feed line length of 500 μm. As can be seen, the designed filter exhibits a low insertion loss of -1.0 dB and good
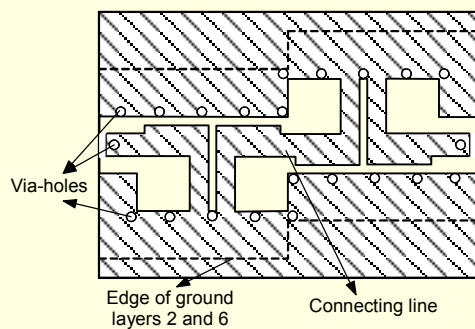
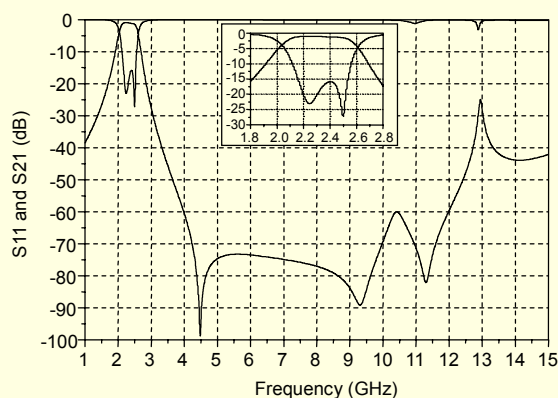Fig. 12. Top view of the cascaded two-stage bandpass filter.

Fig. 14. Photograph of the fabricated bandpass filter mounted on PCB.

Fig. 13. HFSS simulated results of the designed two-stage bandpass filter with a small PCB.
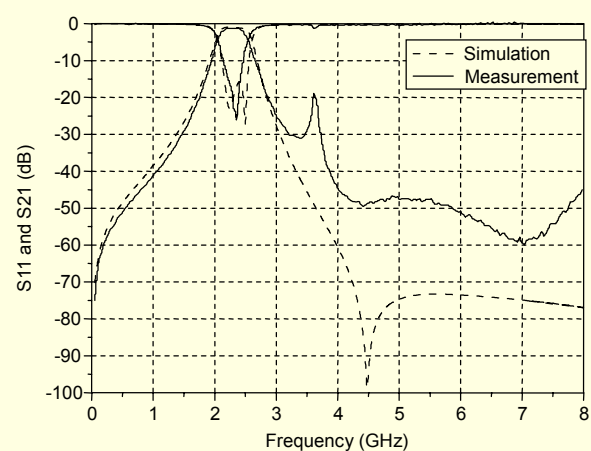
Fig. 15. Comparison of the measured and simulated response.

frequency selectivity. The return loss within the passband is less than -15 dB. Moreover, the rejection level is kept below -40 dB up to 12 GHz, which is 5 times of the center frequency (2.3 GHz), thus making up the attractive ultra-broad rejection of spurious passbands. In particular, due to the transmission zero created by cross-coupling capacitor, the second harmonic attenuation is nearly -80 dB. The filter responses simulated by the full-wave simulator are almost the same as the responses optimized by the circuit simulator ADS. This demonstrates the validity of this design method.

IV. Measurement and Discussion

Having obtained the optimized structural parameters, the chip-type LTCC bandpass filter was fabricated. The dielectric constant of the LTCC raw material is 5.6 ± 0.2 and the conductor is silver with a thickness of 15 μm after firing and conductivity of 5.5×10^7 siemens/m. The via-hole is 200 μm in diameter. Figure 14 shows a photograph of the fabricated bandpass filter mounted on the PCB. The overall size is only 10 mm × 7 mm × 2.2 mm.

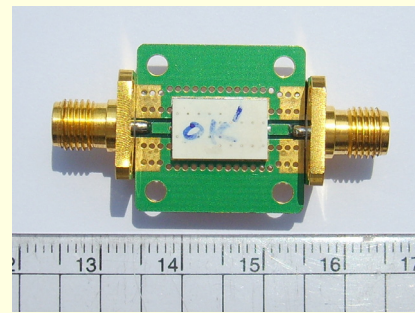The measured responses of the fabricated filter are presented

in Fig. 15 together with the responses from the EM simulation.

The measured center frequency and bandwidth match well with the simulation results. In the passband, the insertion loss is found to be -1.2 dB, and the return loss is better than -15 dB. However, a small unwanted peak at the frequency point of 3.6 GHz appears due to the connecting transmission line. The rejection level at this point is -20 dB. This discrepancy probably comes from the lack of accuracy in the fabrication process. The same phenomenon is seen in Fig. 8. Actually, the printing process is capable of resolving a 150 μm line with 10% accuracy in LTCC technology. Although the out of band rejection is not as excellent as that obtained by the simulation due to the absence of the transmission zero, the average attenuation of -50 dB up to 8 GHz is sufficient.

Since this LTCC bandpass filter was designed to improve the power amplifier efficiency of base stations, it should have high power handling capability. Therefore, a special test was also carried out. It achieved normal operation with a power amplifier of 20 W at 250°C over 24 hours.

Table 2 summarizes the characteristic of several published harmonic suppression filters using the structures of PBG or

Table 2. Comparison of various harmonic-suppression bandpass filters.

Reference	Bandwidth and center frequency (GHz)	S_{11} (dB)	S_{21} (dB)	Harmonic suppression level	Overall physical size (mm×mm)	Technology	Year
[7]	1.85 - 2.15, 2	-	-2.6	Up to 10 GHz, better than -30 dB	120.0 × 30.0	Coupled-line with rectangular PBG loops	2005
[14]	2.9 - 3.1, 3	< -25	-1.5	Up to 6 GHz, better than -40 dB	20.0 × 15.0	Coupled-line with DGS	2002
[19]	3.4 - 5.0, 4.2	< -20	-0.6	Up to 12 GHz, better than -25 dB	10.0 × 5.0	Open-ended stub and DGS	2004
This work	2.18 - 2.42, 2.3	< -15	-1.2	Up to 8 GHz, better than -40 dB	10 × 7 × 2.2	Short-ended coupled-line with capacitive loading and cross-coupling	2009

DGS in comparison with the structure proposed in this work. Obviously, the proposed bandpass filter in this paper shows the advantage of much more compact size and better stopband rejection performance.

V. Conclusion

In this paper, we presented a novel bandpass filter design approach for miniaturization and multi-harmonic suppression using capacitive loading of a parallel coupled-line structure. The method of adding lumped capacitors to the conventional coupled-line section can largely reduce the required length of the coupled-line and effectively suppress spurious passbands. In addition, a cross-coupling capacitor between the input and output ports was introduced into the miniaturized couple-line. It generated a transmission zero to achieve enhanced frequency selectivity and wide multi-harmonic suppression. The aperture compensation technique was also utilized to make a tight coupling under the minimum spacing limitation between the coupled stripline conductors. When cascading two identical one-stage filters, the connecting transmission line between them generated another spurious band. To our knowledge, this was particularly studied for the first time in this paper. The proposed bandpass filter can be made much smaller and achieves an excellent insertion loss compared to the filters using PBG or DGS structures. Moreover, this method is general and geometry-independent; therefore, it can be applied to any type of bandpass filter design. A compact LTCC bandpass filter with a transmission zero at the second harmonic frequency was implemented for experimental demonstration. The measured and simulated results show good agreement, which demonstrates that the proposed filter has great application potential.

References

[1] A.B. Frazier, R.O. Warringtun, and C. Friedrich, "The Miniaturization Technologies: Past, Present, and Future," *IEEE Trans. Ind. Electron.*, vol. 42, Oct. 1995, pp. 423-430.

[2] K.L. Tai, "System-in-Package (SiP): Challenges and Opportunities," *Proc. Asia–South Pacific Design Automation Conf.*, 2000, pp. 191-196.

[3] A. Matsuzawa, "RF-SoC: Expectations and Required Conditions," *IEEE Trans. Microwave Theory and Tech.*, vol. 50, no. 1, Jan. 2002, pp. 245-253.

[4] J. Muller and H. Thust, "3D-Intergration of Passive RF-Components in LTCC," *Pan Pacific Microelectronic Symp. Dig.*, 1997, pp. 211-216.

[5] C.Q. Scrantom and J.C. Lawson, "LTCC Technology: Where We Are and Where We're Going—II," *IEEE MTT-S Int. Microwave Symp.*, Dig., 1999, pp. 193-200.

[6] I. Rumsey, M. Piket-May, and P. Kelly, "Photonic Bandgap Structures Used as Filters in Microstrip Circuits," *IEEE Microw. Guided Wave Lett.*, vol. 8, no. 10, Oct. 1998, pp. 336-338.

[7] M.H. Weng et al., "Spurious Suppression of a Microstrip Bandpass Filter Using Three Types of Rectangular PBG Loops," *IEEE Trans. Ultrasonics, Ferroelectrics, and Frequency Control*, vol. 52, no. 3, Mar. 2005, pp. 487-490.

[8] T. Kim and C. Seo, "A Novel Photonic Bandgap Structure for Low-Pass Filter of Wide Stopband," *IEEE Microw. Guided Wave Lett.*, vol. 10, no. 1, Jan. 2000, pp. 13-15.

[9] J. Yoon and C. Seo, "Improvement of Broadband Feedforward Amplifier Using Photonic Bandgap," *IEEE Microw. Wireless Compon. Lett.*, vol. 11, no. 11, Nov. 2001, pp. 450-452.

[10] D. Ahn et al., "A Design of the Low-Pass Filter Using the Novel Microstrip Defected Ground Structure," *IEEE Trans. Microwave Theory and Tech.*, vol. 49, no. 1, Jan. 2001, pp. 86-93.

[11] J.S. Lim et al., "Application of Defected Ground Structure in Reducing the Size of Amplifiers," *IEEE Microw. Wireless Compon. Lett.*, vol. 12, no. 7, July 2002, pp. 261-263.

[12] J.S. Lim et al., "A 4:1 Unequal Wilkinson Power Divider," *IEEE Microw. Wireless Compon. Lett.*, vol. 11, no. 3, Mar. 2001, pp. 124-126.

[13] D. Guha, M. Biswas, and Y.M.M. Antar, "Microstrip Patch Antenna with Defected Ground Structure for Cross Polarization Suppression," *IEEE Antennas and Wireless Propagation Lett.*, vol. 4, no. 1, 2005, pp. 455-458.

[14] J.S. Park, J.S. Yun, and D. Ahn, "A Design of the Novel Coupled Line Bandpass Filter Using Defected Ground Structure with Wide Stopband Performance," *IEEE Trans. Microwave Theory and Tech.*, vol. 50, no. 9, Sept. 2002, pp. 2037-2043.

[15] I.H. Kang and J.S. Park, "A Reduced-Size Power Divider Using the Coupled Line Equivalent to a Lumped Inductor," *Microwave Journal*, vol. 46, no. 7, July 2003.

[16] D.M. Pozar, *Microwave Engineering*, 2nd ed., Addison-Wesley, New York, 1998.

[17] I.H. Kang and H.Y. Xu, "An Extremely Miniaturized Microstrip Bandpass Filter," *Microwave Journal*, vol. 50, no. 5, May 2007, pp. 228-233.

[18] I.H. Kang and K. Wang, "A Broadband Rat-Race Ring Coupler with Tightly Coupled Lines," *IEICE Trans. Commun.*, vol. E88-B, no. 10, Oct. 2005, pp. 4087-4089.

[19] A. Abdel-Rahman et al., "Compact Stub Type Microstrip Bandpass Filter Using Defected Ground Plane," *IEEE Microw. Wireless Compon. Lett.*, vol. 14, no. 4, Apr. 2004, pp. 136-138.

Xu-Guang Wang received his BS degree in electronic engineering from Qingdao University, Qingdao, China, in 2006, and the MS degree in radio science and engineering from Korea Maritime University, Busan, Korea, in 2008. He is currently working toward the PhD with the Department of Electronic Engineering, Sogang University, Seoul, Korea. His research interests include the design of microwave filters and associated RF modules for microwave and millimeter-wave applications.

Young Yun received his BS degree in electronic engineering from Yonsei University, Seoul, Korea, in 1993; the MS degree in electrical and electronic engineering from Pohang University of Science and Technology, Pohang, Korea, in 1995; and his PhD in electrical engineering from Osaka University, Osaka, Japan, in 1999. From 1999 to 2003, he worked as an engineer with Matsushita Electric Industrial Co. Ltd., Osaka, Japan, where he was engaged in the research and development of MMICs for wireless communications. In 2003, he joined the Department of Radio Science and Engineering, Korea Maritime University, Busan, Korea, where he is now an assistant professor. His research interests include the design and measurement of RF/microwave and millimeter-wave ICs, and the design and fabrication of HEMTs and HBT.

In-Ho Kang received his PhD in electronic engineering from Sogang University, Seoul, Korea, in 1995. He was a visiting professor at Cardiff University, Cardiff, UK, in 2008. He is now a professor with the Department of Radio Science and Engineering, Korea Maritime University, Busan, Korea. His research interests include CMOS MMIC filters for RF single chips for the 2.4 and 5.5 GHz bands, WiMAX and UWB applications, and MMIC filters for power amplifier harmonics suppression.